Supporting Information

Probing nanoscale diffusional heterogeneities in cellular membranes through multidimensional single-molecule and super-resolution microscopy

Rui Yan, Kun Chen, Ke Xu*

Department of Chemistry, University of California, Berkeley, CA 94720

Chan Zuckerberg Biohub, San Francisco, CA 94158

*Correspondence to: xuk@berkeley.edu

Materials and Methods

Dye characterization. BDP-TMR-alkyne (A24B0, Lumiprobe) was prepared as an 1 mM stock solution in DMSO, and diluted to 0.2-1.0 μM in different solvents for absorbance and fluorescence quantum-yield measurements (Figure S1), and 3.3 nM in ethanol or the cell imaging buffer (below) for fluorescence measurements under conditions comparable to the single-molecule experiments (Figure 1b). For measurement of quantum yield, Rhodamine 6G (252433, Sigma-Aldrich) was diluted to 0.2-1.0 μM in ethanol as the standard, for its well-characterized quantum yield of 95% under 530-nm excitation (Brouwer 2011). Fluorescence emission was recorded using a Duetta spectrometer (HORIBA Instruments), with excitation at 530 nm (Figure S1bd) or 560 nm (Figure 1b). Absorption spectra were recorded using the same cuvettes on a NanoDrop 2000c spectrometer (Thermo Fisher) in the cuvette mode, with background subtraction at 750 nm.

Cell culture. COS-7 cells (University of California Berkeley Cell Culture Facility) were maintained in Dulbecco's Modified Eagle Medium supplemented with 10% fetal bovine serum and 1% non-essential amino acids. Two days prior to imaging, cells were plated onto 18-mm diameter glass coverslips that were pretreated with hot piranha solutions (H_2SO_4:H_2O_2 at 3:1). Transfection of GRAMD1a-AcGFP and GRAMD2a-AcGFP [kind gifts from Prof. Jodi Nunnari (Besprozvannaya *et al.* 2018)] was performed one day after plating. 300-500 ng plasmid was used per sample with the standard Lipofectamine 3000 protocol (Thermo Fisher). Before imaging, the coverslip was transferred to a holder (CSC-18, Bioscience Tools) compatible with the microscope stage. Imaging medium was Leibovitz's L-15 or a MOPS-based buffer (Hibernate A Low Fluorescence, BrainBits), with similar results observed. BDP-TMR-alkyne or Nile Red (Acros Organics) was diluted into the imaging medium to a final concentration of 3.3 nM. The dye-added imaging medium was added to the sample and remained unchanged throughout imaging. For CTB treatment, cells were incubated with 1 μg/mL Alexa Fluor 488-conjugated CTB (C34775, Invitrogen) in the culture medium for ~5 min, and then washed twice with the imaging medium before imaging.

Concurrent SM*d*M and 3D-SMLM. Concurrent SM*d*M and 3D-SMLM of BDP-TMR-alkyne was achieved *via* modifications to a homebuilt system (Wojcik *et al.* 2015) based on a Nikon Eclipse Ti-E inverted optical microscope. Lasers at 488, 560, and 647 nm were independently modulated by an acousto-optic tunable filter (97-03151-01, Gooch & Housego) that was driven by an 8-channel RF synthesizer (97-03926-12, Gooch & Housego). The modulated laser beams were focused onto the back focal plane of an oil-immersion objective lens (Nikon CFI Plan Apochromat λ 100x, numerical aperture: 1.45) toward the edge, thus entering the sample slightly below the critical angle to illuminate a ~1 μm depth. For 3D localization, a cylindrical lens was used to induce elongations of single-molecule images in the vertical and horizontal directions for molecules below and above the focal plane, respectively (Huang *et al.* 2008). The focal plane was set ~200 nm into the sample, so that depth (z) values of ~−200 nm corresponded to the substrate. Single-molecule images due to the transient entrance of individual BDP-TMR-alkyne molecules into the membrane phase (Sharonov and Hochstrasser 2006) were continuously recorded in the wide-field using an EM-CCD camera (iXon Ultra 897, Andor) at a fixed frame rate of 110 fps. A multifunction I/O board (PCI-6733, National Instruments) read the camera exposure timing signal, and accordingly modulated the RF synthesizer to achieve frame-synchronized stroboscopic excitation for the 560 nm laser in two modes. In the

first mode, paired pulses of τ = ~1 ms duration and Δt = 2.5 ms center-to-center separation were repeatedly applied across tandem camera frames (Figure 1g inset), so that single-molecule images from the paired odd-even frames captured transient displacements in the Δt time window (Xiang *et al.* 2020). In the second mode, pulses of τ = 0.5-2 ms duration were applied at the middle of each frame (Figure 1h inset). Single-molecule displacements were thus assessed between consecutive frames for Δt = 9.1 ms displacement time. The estimated peak and average power densities of the excitation laser at the sample were ~10 and ~1 kW/cm^2, respectively. 90,000-160,000 frames of single-molecule images were recorded under the above stroboscopic excitation schemes, from which 10^6–10^7 molecules were accumulated across the view. The 488 nm laser was separately applied before and/or after the above stroboscopic single-molecule experiments for epifluorescence imaging of AF488-tagged CTB and GFP-tagged GRAMD1a and GRAMD2a.

Concurrent SM*d*M and SR-SMLM. Concurrent SM*d*M and SR-SMLM of Nile Red were achieved on another homebuilt system as described previously (Moon *et al.* 2017; Xiang *et al.* 2020). Briefly, frame-synchronized stroboscopic excitation was achieved through direct power modulation of the 561 nm laser (OBIS 561 LS, Coherent) using a multifunction I/O board (PCI-6733, National Instruments) (Xiang *et al.* 2020). Paired pulses of τ = 2 ms duration and Δt = 2.5 ms center-to-center separation were repeatedly applied across tandem camera frames for evaluation of single-molecule displacements from the paired odd-even frames. The estimated peak and average power densities of the excitation lasers at the sample were ~6 and ~1 kW/cm^2, respectively. Single-molecule emission due to the transient entrance of individual Nile Red molecules into the membrane phase (Sharonov and Hochstrasser 2006) was split 50:50 for the concurrent recording of the unmodified images and the dispersed emission spectra in the wide-field (Moon *et al.* 2017). An EM-CCD camera (iXon Ultra 897, Andor) recorded ~120,000 frames at 110 fps.

3D-SMLM of GRAMD1a and GRAMD2a. For 3D-SMLM of GRAMD1a-AcGFP and GRAMD2a-AcGFP, transfected cells were fixed by 3% paraformaldehyde and 0.1% glutaraldehyde in phosphate-buffered saline (PBS) for 20 min, followed by a 5-min wash with freshly prepared 0.1% $NaBH_4$ in PBS. The sample was washed 3 times with PBS, and immunolabeled with a mouse anti-GFP primary antibody (Invitrogen A11120) and an Alexa Fluor 647-labeled secondary antibody (Invitrogen A21236). The labeled samples were imaged in a photoswitching buffer (100 mM Tris-HCl pH 7.5, 100 mM cysteamine, 5% glucose, 0.8 mg/mL glucose oxidase, and 40 μg/mL catalase) on the 3D-SMLM setup described above. ~50,000 frames of single-molecule images were recorded at 110 fps under continuous 647-nm excitation.

Data analysis. Single-molecule raw images were first localized and rendered into 3D-SMLM images as described in (Rust *et al.* 2006; Huang *et al.* 2008). SR-SMLM data were processed as described in (Moon *et al.* 2017; Zhang *et al.* 2015). SM*d*M analysis under the isotropic diffusion model was performed as described in (Xiang *et al.* 2020). Briefly, the accumulated single-molecule displacements were spatially binned into 100×100 nm^2 bins. The displacements in each spatial bin were then separately fitted to a modified isotropic 2D random-walk model with the probability distribution

$$P(r) = \frac{2r}{a}\exp(-\frac{r^2}{a}) + br \quad \text{(eqn. 1)}$$

where r is the single-molecule displacement in the fixed time interval Δt, $a = 4D\Delta t$, and b is a background term to account for molecules that randomly enter the view, as rationalized and validated in (Xiang *et al.* 2020) with experiments carried out at different single-molecule densities. For the pSM*d*M analysis, for each spatial bin, we first calculated the angular coordinate φ of each single-molecule displacement accumulated in the bin. As we consider molecules traveling in opposite directions to be diffusing along the same axis, we first flipped all displacements with φ in the range of (-180°, 0°) by adding 180°, so that all the resultant φ' values were in the range of [0°, 180°]. We then took the circular mean of $2\varphi'$ (in the range of [0°, 360°]) for all displacements in the spatial bin, and divided this value by 2 to obtain the average direction of diffusion θ (principal direction). Anisotropy α is also assessed in the process by dividing the modulus of the vector sum (in the $2\varphi'$ angle space) over the sum of the moduli of all the displacements, hence a value of 0 and 1 for fully isotropic and fully anisotropic (bidirectional along a line) diffusions, respectively. Results at each spatial bin were converted into a color for color-map presentation (*e.g.*, Figure 3g and Figure S2) *via* the HSV (hue, saturation, value) color space, with hue, saturation, and value corresponding to θ, α, and single-molecule count, respectively. The single-molecule displacements in each bin were next separately projected along and perpendicular to the calculated θ direction (*e.g.*, Figure 3bcef) for fitting to a modified 1D random-walk model with the probability distribution of $P(x) = \frac{1}{\sqrt{a\pi}} \exp(-\frac{x^2}{a}) + b'$ (Xiang *et al.* 2020), where $a = 4D\Delta t$. The larger resultant D value of the two was picked to generate pSM*d*M color maps.

References

Besprozvannaya, M., Dickson, E., Li, H., Ginburg, K. S., Bers, D. M., Auwerx, J., and Nunnari, J., 2018. "GRAM domain proteins specialize functionally distinct ER-PM contact sites in human cells." *eLife*, **7**: e31019.

Brouwer, A. M., 2011. "Standards for photoluminescence quantum yield measurements in solution (IUPAC technical report)." *Pure Appl. Chem.*, **83**: 2213-2228.

Cser, A., Nagy, K., and Biczók, L., 2002. "Fluorescence lifetime of Nile Red as a probe for the hydrogen bonding strength with its microenvironment." *Chem. Phys. Lett.*, **360**: 473-478.

Davis, M. M., and Helzer, H. B., 1966. "Titrimetric and equilibrium studies using indicators related to nile blue A." *Anal. Chem.*, **38**: 451-461.

Huang, B., Wang, W., Bates, M., and Zhuang, X., 2008. "Three-dimensional super-resolution imaging by stochastic optical reconstruction microscopy." *Science*, **319**: 810-813.

Moon, S., Yan, R., Kenny, S. J., Shyu, Y., Xiang, L., Li, W., and Xu, K., 2017. "Spectrally resolved, functional super-resolution microscopy reveals nanoscale compositional heterogeneity in live-cell membranes." *J. Am. Chem. Soc.*, **139**: 10944-10947.

Rust, M. J., Bates, M., and Zhuang, X., 2006. "Sub-diffraction-limit imaging by stochastic optical reconstruction microscopy (STORM)." *Nat. Methods*, **3**: 793-795.

Sharonov, A., and Hochstrasser, R. M., 2006. "Wide-field subdiffraction imaging by accumulated binding of diffusing probes." *Proc. Natl. Acad. Sci. U. S. A.*, **103**: 18911-18916.

Wojcik, M., Hauser, M., Li, W., Moon, S., and Xu, K., 2015. "Graphene-enabled electron microscopy and correlated super-resolution microscopy of wet cells." *Nat. Commun.*, **6**: 7384.

Xiang, L., Chen, K., Yan, R., Li, W., and Xu, K., 2020. "Single-molecule displacement mapping unveils nanoscale heterogeneities in intracellular diffusivity." *Nat. Methods*, **17**: 524-530.

Zhang, Z., Kenny, S. J., Hauser, M., Li, W., and Xu, K., 2015. "Ultrahigh-throughput single-molecule spectroscopy and spectrally resolved super-resolution microscopy." *Nat. Methods*, **12**: 935-938.

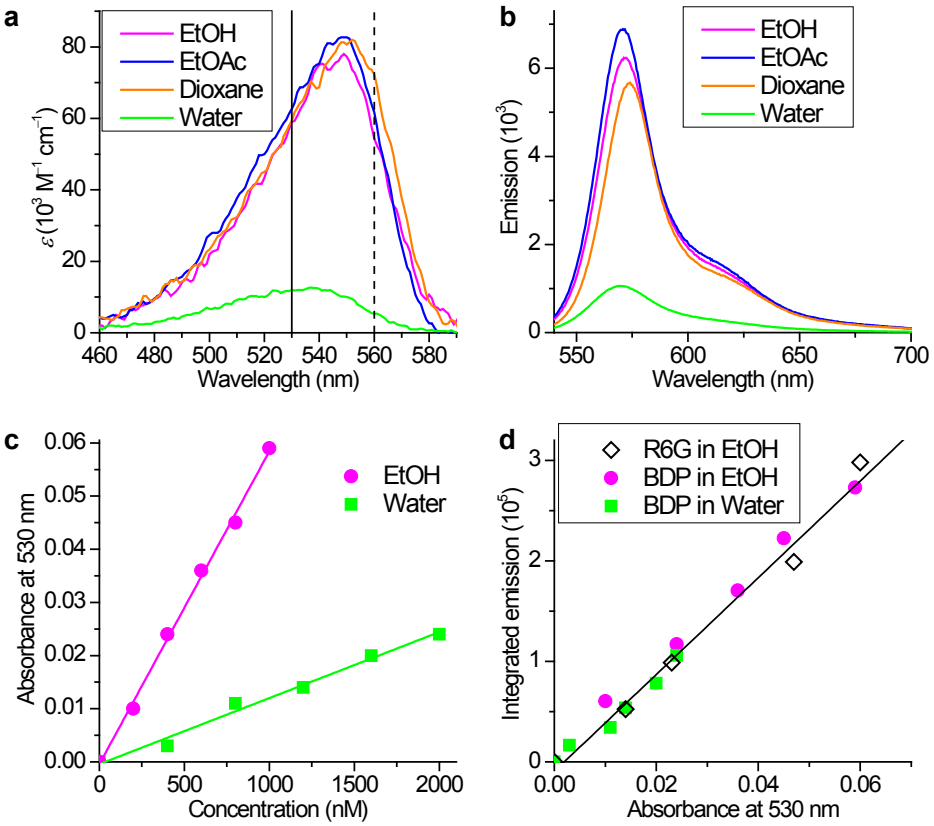

Figure S1. Spectral properties of BDP-TMR-alkyne in different solvents. (a) Absorption spectra of 1 μM BDP-TMR-alkyne in different solvents. Comparable results are found for three organic solvents of varying chemical polarities (ethanol, ethyl acetate, and 1,4-dioxane), yet the absorption in water is noticeably reduced and blue-shifted. The solid and dashed vertical lines correspond to excitation wavelengths used to determine quantum yields below (530 nm), and used in our single-molecule experiments and Figure 1b (560 nm), respectively. (b) Fluorescence emission spectra of 1 μM BDP-TMR-alkyne in different solvents when excited at 530 nm, showing comparable results between the three organic solvents but much lower emission in water. (c) Absorbance of BDP-TMR-alkyne at 530 nm as a function of concentration, in ethanol vs. in water. Lines: linear fits to data. (d) Emission as a function of absorbance at 530 nm, for BDP-TMR-alkyne of varied concentrations in ethanol vs. in water [same absorbance values as shown in (c)], in comparison to that of Rhodamine 6G (R6G) in ethanol. Line: a linear fit to the R6G data. Similar emission-absorbance trends are found for all three systems, indicating that the fluorescence quantum yields (QY) of BDP-TMR-alkyne in ethanol and in water are both comparable to that of R6G in ethanol, which has a known QY of 95% (Brouwer 2011). Thus, the substantially reduced fluorescence emission of BDP-TMR-alkyne in the aqueous phase under 560 nm excitation (Figure 1b) is due to reduced and blue-shifted absorption, rather than due to a significant change in QY. Meanwhile, the measured higher QY (~95%) and extinction coefficients [ε~80,000 $M^{-1}cm^{-1}$ from (a)] of BDP-TMR-alkyne in organic solvents when compared to Nile Red (QY~50-80% and ε~38,000 $M^{-1}cm^{-1}$) (Davis and Helzer 1966; Cser *et al.* 2002) justify its superior single-molecule photon counts in cellular membranes.

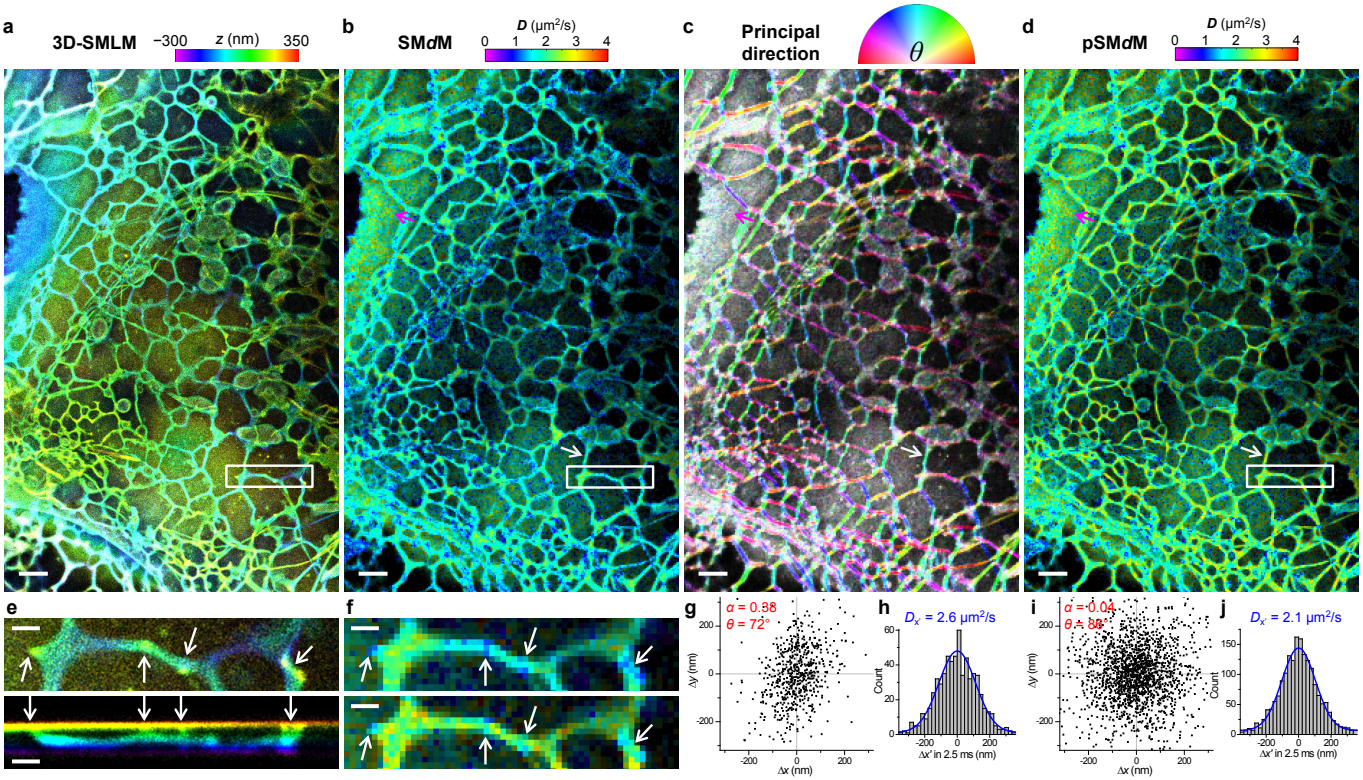

Figure S2. Additional stroboscopic PAINT and SM*d*M results of BDP-TMR-alkyne on a COS-7 cell, acquired with tandem excitation pulses of τ = 1.5 ms duration and Δt = 2.5 ms center-to-center separation. (a) 3D-SMLM image constructed from the single-molecule positions. Color presents depth (color scale on the top). (b) SM*d*M diffusivity map constructed from the single-molecule displacements of the same data, based on an isotropic 2D fitting model. Color presents D value (color scale on the top). (c) Principal direction (θ) - anisotropy (α) color map of the diffusion data. Hue, saturation, and value present θ, α, and single-molecule count, respectively. (d) pSM*d*M diffusivity map after the principal-direction analysis. (e) Zoom-in of the white box in (a) (top), and its cross-sectional view in the *xz* direction (bottom). (f) Isotropic SM*d*M (top) and pSM*d*M (bottom) diffusivity maps of the same region. White arrows point to possible ER-PM contact sites. (g) 2D plot of single-molecule displacements in 2.5 ms for BDP-TMR-alkyne at an ER tubule [white arrows in (b-d)]. A principal direction θ of 72° is calculated with an anisotropy α of 0.38. (h) 1D distribution of the displacements in (g) projected along θ. Blue curve: MLE fit to a 1D diffusion model with resultant D = 2.6 μm^2/s. (i) 2D plot of single-molecule displacements in 2.5 ms for BDP-TMR-alkyne at the plasma membrane [magenta arrows in (b-d)]. α = 0.04 and θ = 86°. (j) 1D distribution of the displacements in (i) projected along θ. Blue curve: MLE fit to a 1D diffusion model with resultant D = 2.1 μm^2/s. Scale bars: 2 μm (a-d); 500 nm (e,f).

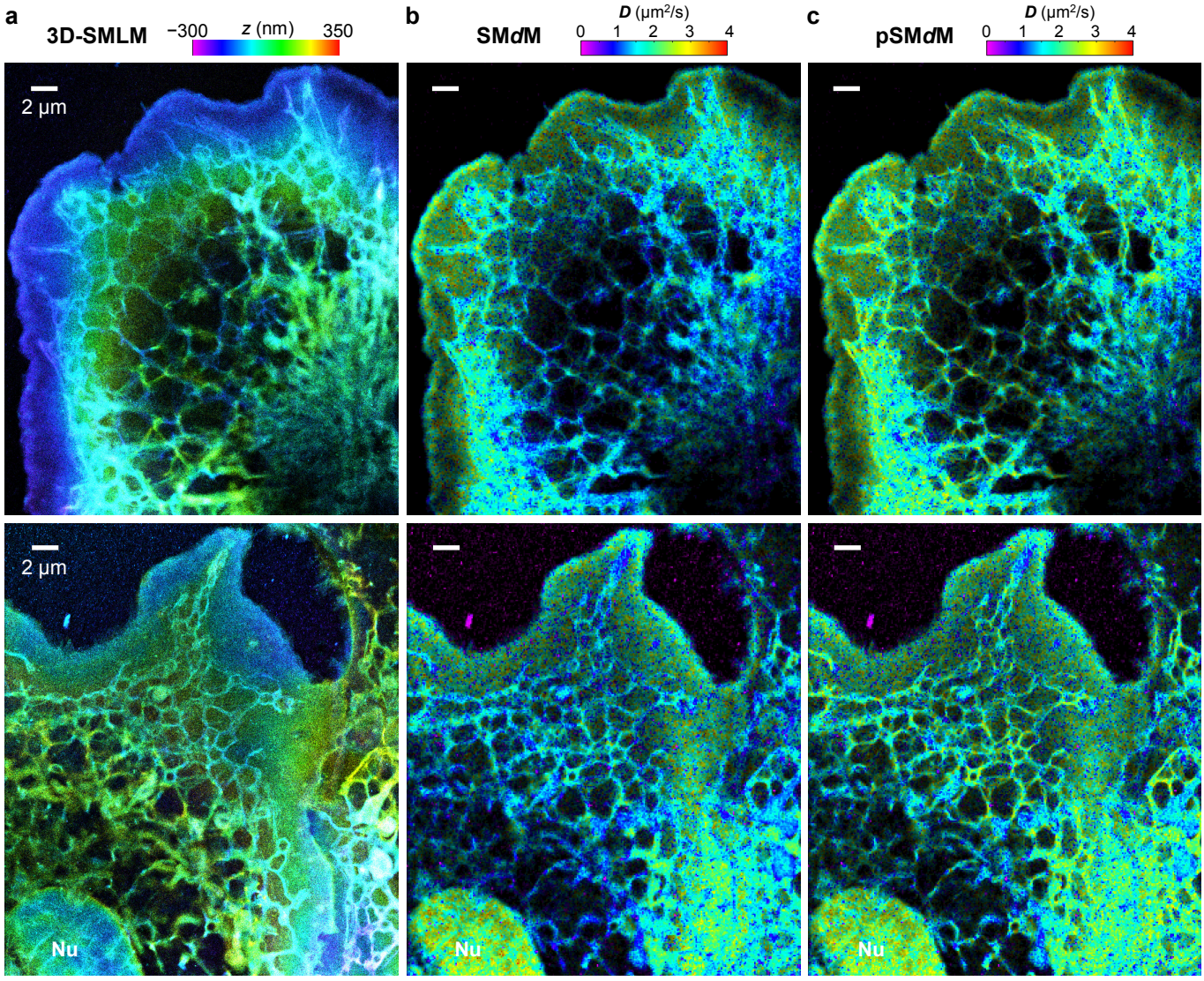

Figure S3. Additional stroboscopic PAINT and SM*d*M results of BDP-TMR-alkyne on COS-7 cells, acquired with stroboscopic excitations at the middle of every frame (Δt = 9.1 ms), with excitation pulses of τ = 0.5 ms (top) and 2 ms (bottom) durations, respectively. (a) 3D-SMLM image. Color presents depth (color scale on the top). (b,c) Isotropic SM*d*M (b) and pSM*d*M (c) diffusivity maps. Color presents *D* value (color scale on the top).

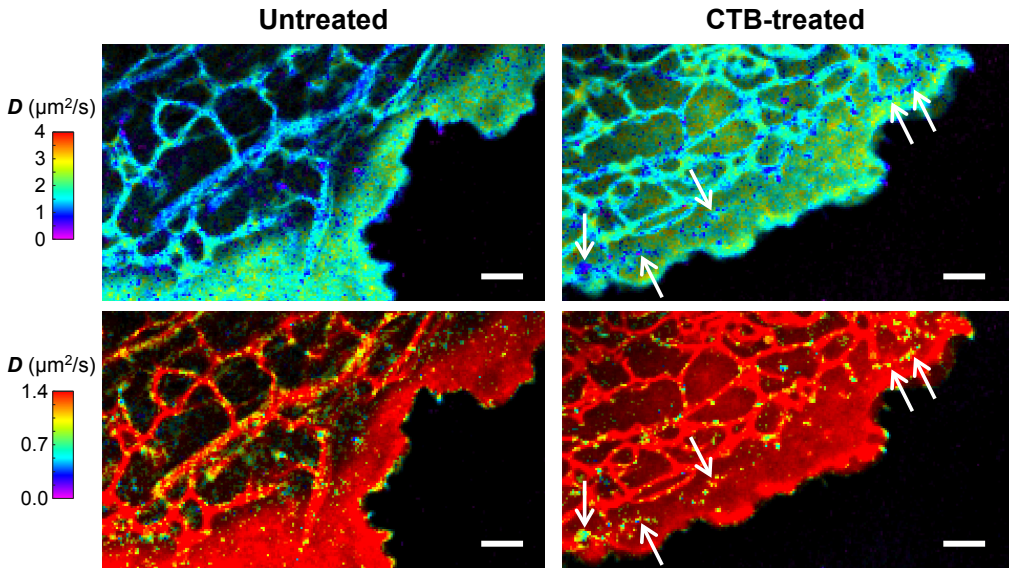

Figure S4. Side-by-side comparison of the SM*d*M results of BDP-TMR-alkyne in untreated and CTB-treated COS-7 cells, presented on the original *D* color scale of 0-4 μm^2/s as Figure 2ce (top row), and on a substantially reduced *D* scale of 0-1.4 μm^2/s (bottom row). An increased appearance of nanoscale foci of very low diffusivity is found after the CTB treatment, and many of these foci colocalized with the CTB fluorescence (arrows; see also Figure 2d). Additional low-diffusivity foci are observed at potential ER-PM contact sites for both samples. Scale bars: 2 μm.